Electrical properties of percolation clusters: exact results on a deterministic fractal

1985 J. Phys. A: Math. Gen. 18 2565

(http://iopscience.iop.org/0305-4470/18/13/032)

J. Phys. A: Math. Gen. **18** (1985) 2565-2582. Printed in Great Britain

Electrical properties of percolation clusters: exact results on a deterministic fractal

J P Clerc†, G Giraud†, J M Laugier† and J M Luck‡

† Département de Physique des Systèmes Désordonnés, Université de Provence, Centre de St Jérôme, 13397 Marseille Cedex 13, France
‡ SPHT, CEN Saclay, BP 2, 91191 Gif-sur-Yvette Cedex, France

Received 6 November 1984, in final form 8 March 1985

Abstract. A recursively built deterministic fractal lattice, generalising a model proposed by Kirkpatrick, is used to examine general electrical properties of percolation clusters in arbitrary dimension. Most physical quantities are exactly analytically tractable, since the model admits an exact renormalisation group transformation, associated with a rational mapping $T(x)$ of one complex variable. The model has one free parameter f, the fraction of conducting material, which is put equal to the self-dual point $f=\frac{2}{3}$ in two dimensions, and chosen to reproduce the numerical values of the exponent ratio t/ν in higher dimensions.

Our results concern in particular the frequency dependence of the impedance and the loss angle, where we prove the existence of scaling laws at low and high frequency. We also determine exactly the transient response to an arbitrary input signal, and relate the distribution of relaxation times of the infinite lattice to well known mathematical objects associated to the rational transform T, namely its Julia set and its invariant measure. The critical amplification of flicker (or $1/f$) resistor noise is also considered; it is shown to obey scaling laws with its own critical exponents, in agreement with other recent works. The relationships to other theoretical models and to experiments on metal-insulator mixtures are discussed.

1. Introduction

The electrical properties of random media near their percolation threshold have been the subject of much interest. The analogy between percolation and continuous phase transitions has been extended to dynamical quantities, such as the conductivity σ and the dielectric constant ε (see Kirkpatrick 1978, 1979, Stauffer 1979, Essam 1980 for reviews). These quantities obey the following scaling laws: $\sigma \sim (p-p_c)^t$ $(p>p_c)$ and $\varepsilon \sim |p_c-p|^{-s}$, where the critical exponents s and t are not related to the static ones, just as in the area of critical dynamics. The numerical values of s and t are known with a good accuracy in dimensions 2 and 3:

$$s/\nu(2D) = t/\nu(2D) = 0.977 \pm 0.010$$

$$s/\nu(3D) = 0.85 \pm 0.04 \qquad t/\nu(3D) = 2.20 \pm 0.10$$

(Derrida *et al* 1983a, Herrmann *et al* 1984, Hong *et al* 1984, Zabolitzky 1984, Lobb and Franck 1984).

Percolation is certainly the example of critical phenomena where the critical exponents and anomalous dimensions have the most concrete interpretation in terms

of Hausdorff (or fractal) dimensions of several objects: the infinite cluster itself, its 'backbone', or the random walk on these sets. A lot of attention has been paid to this approach (Kirkpatrick 1979, Gefen *et al* 1981, Alexander and Orbach 1982, Rammal and Toulouse 1983, Stanley and Coniglio 1984, Herrmann and Stanley 1984).

Inhomogeneous deterministic fractals, usually built recursively, have also been used to mimic some properties of percolation clusters (Kirkpatrick 1979, Gefen *et al* 1981, Rammal and Toulouse 1983, Clerc *et al* 1984). Their main advantage is that they allow for exact analytical treatments. In the present paper, we aim to use such a fractal lattice to study general electrical properties of percolation clusters, like the frequency dependence of the impedance, as well as transient regimes and noise amplification.

The fractal set we have chosen to work with has been proposed by Kirkpatrick (1979). It is also described in Mandelbrot (1982). It is obtained by cutting off a quarter of a square conducting sheet, then a randomly chosen quarter of each of the three remaining squares, and so on. Figure 1 shows the first three steps of that construction. We propose to generalise it by allowing for a conducting fraction f different from Kirkpatrick's original choice $f=\frac{3}{4}$, and to replace the holes by perfect capacitors. Figure 2 shows the equivalent circuit at generation $n=0$, 1 and 2 (for $f=\frac{3}{4}$). Let us mention that the Kirkpatrick representation is ambiguous (are two neighbouring squares in electrical contact?), while the network representation clearly defines which connections are present and which are not. A remarkable feature of this model is that

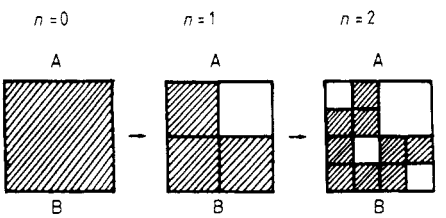

Figure 1. The first three steps of Kirkpatrick's original construction of a 2D fractal imitating a percolation backbone.

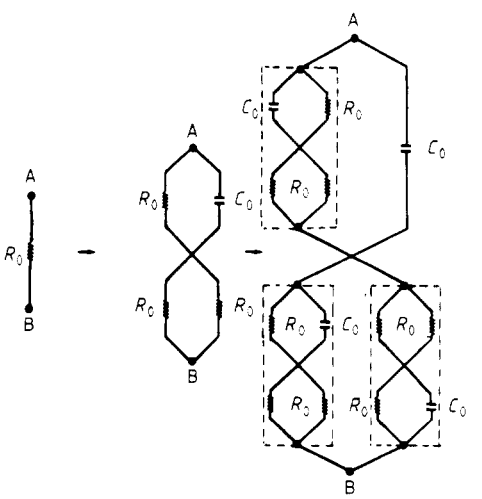

Figure 2. The circuit representation of the 2D deterministic fractal lattice at generation $n=0$, 1 and 2, for $f=\frac{3}{4}$.

the properties of the lattice are independent of the choice of random positions of resistors and capacitors inside each cell: only their number matters.

In order to realise a lattice with a value of f different from $\frac{3}{4}$, one just allows the number of capacitors per unit cell to be $4(1-f)$ instead of 1. In other words, one half of each cell (the upper half, say) contains $4(1-f)$ capacitors and $(4f-2)$ resistors in parallel, while the lower half contains two resistors in parallel. The fact that this number is generally not an integer is harmless: f has only to satisfy $\frac{1}{2}<f<1$. In the following, we shall denote by DFL this f-dependent deterministic fractal lattice.

The plan of the article is as follows. In § 2, we show how the frequency-dependent impedance of the DFL may be related to the iterates of a given rational transformation T, which will play a central role throughout the paper. We study in detail the crossover behaviours of the impedance at low and high frequency, as well as the loss angle. The construction of the DFL is generalised to dimensionalities higher than 2, with emphasis on the 3D case. In § 3, we determine the transient response of the DFL to an arbitrary input signal, and show how the intrinsic relaxation times of the network are related to the Julia set of the mapping T. In § 4, we compute the frequency dependence of the amplification of the microscopic flicker-type resistor noise by the fractal structure of the DFL. The relationships of our model to more realistic cases, as well as its limitations, are discussed in § 5.

2. Frequency dependence of the impedance and the loss angle

2.1. Two-dimensional case

Consider the DFL of figure 2 at the generation number n (it has 4^n bonds). Let R_0 be the resistance of the conducting bonds and C_0 the capacitance of the insulating ones. The frequency-dependent impedance $Z_n(\omega)$ of the lattice between points A and B satisfies the following recursion relation:

$$Z_n(\omega)=\tfrac{1}{2}Z_{n-1}(\omega)+\left(\frac{4(1-f)}{\zeta(\omega)}+\frac{4f-2}{Z_{n-1}(\omega)}\right)^{-1} \tag{2.1}$$

where $\zeta(\omega)=(\mathrm{i}C_0\omega)^{-1}$ is the impedance of an insulating bond. This equation can be iterated down to $n=0$, where we have $Z_0=R_0$, and hence we easily obtain:

$$Z_n(\omega)=(\mathrm{i}C_0\omega)^{-1}T^n(\mathrm{i}\omega/\omega_0) \tag{2.2}$$

where $\omega_0=(R_0C_0)^{-1}$ is the microscopic frequency scale of the lattice, and $T^n=T\circ T\circ\ldots\circ T$ (n times) is the nth iterate of the following rational transformation:

$$T(x)=x\frac{(1-f)x+f}{2(1-f)x+2f-1}. \tag{2.3}$$

The study of the sequence of impedances $Z_n(\omega)$ is therefore reduced to that of the iterations of one single rational function T, which can be viewed as a renormalisation group transformation of the impedance ratio x. This type of rational renormalisation mappings in one variable has been recently studied in the context of hierarchical Potts models (Derrida *et al* 1983a, Derrida *et al* 1984, Itzykson and Luck 1983).

The mapping T contains a lot of information on the electrical properties of the DFL. It will be emphasised in the following that a given feature of the transformation T or of its iterates corresponds to each electrical characteristic of our lattice.

Let us first analyse the fixed points of T: there are three such points (satisfying $T(x)=x$), namely: $x=0$, $x=1$ and $x=\infty$. It is soon realised that $x=1$ is the only *stable* fixed point of T, corresponding to a *pure medium* (since $x_0=1$ means that each bond has the same impedance). The two other fixed points are *unstable*: as could be expected, the DFL exhibits *critical* properties for $\omega\to 0$ and $\omega\to\infty$. Let us repeat once more that these results hold only for $\frac{1}{2}<f<1$.

Before studying equation (2.2) in more detail, we need some mathematical results concerning the iterates of the mapping T. The following is necessary to understand in detail the properties of our DFL, although it will appear technical and unattractive to the non-mathematician reader, since the main advantage of the present model is to be exactly solvable.

Let us first show briefly that the fixed point $x=1$ of the renormalisation mapping T is its unique attractor (using the terminology of dynamical systems). To do so we have to determine the *critical points* of T, defined in the mathematical literature as being those (complex) values of x where the derivative $\mathrm{d}T/\mathrm{d}x$ vanishes. They read:

$$x_\pm=\frac{1-2f\pm \mathrm{i}(2f-1)^{1/2}}{2(1-f)}. \tag{2.4}$$

These have nothing to do with critical phenomena in the physical sense, which occur at 0 and ∞. We know from the theory of rational transformations (Julia 1918, Fatou 1919, 1920, Brolin 1965) that the basin of each attractor contains at least one critical point. This, together with the existence of a stable real fixed point $x=1$, and the fact that $x_\pm$ given by (2.4) are complex conjugates of each other, ensures that the fixed point $x=1$ is the only attractor of T. Another consequence of the unicity of the attractor is the structure of the associated *Julia set* J. In the present case, J can be defined as being the set of points x for which $T^n(x)$ does not go to one as $n\to\infty$. For instance J contains the unstable fixed points 0 and ∞. This Julia set, which has just been defined in a rather abstract fashion, will receive a physical interpretation in § 3 in terms of the transient response of the DFL to an arbitrary signal. In the above mentioned work on the hierarchical Potts model, the Julia set also has an interpretation in terms of physical quantities: it is the locus of the zeros of the partition function. Let us now give a simple explicit construction of this set J. For a generic complex number x, there are *two* complex numbers $y_\pm$ such that $T(y_\pm)=x$. These are called the *pre-images* of $T_\pm^{-1}(x)$. They read:

$$T_\pm^{-1}[x]=\frac{2(1-f)x-f_\pm[4(1-f)^2x(x-1)+f^2]^{1/2}}{2(1-f)}. \tag{2.5}$$

The iterated pre-images $T^{-n}(x)$ are defined for every integer n as being the 2^n numbers y such that $T^n(y)=x$. It is known that the Julia set J is the accumulation set of $T^{-n}(x_0)$ for a generic x_0. It is soon realised from (2.5) that, whenever x is a real negative number, its pre-images $T_\pm^{-1}(x)$ are also real negative. The set J is therefore contained in the negative real axis. Moreover, we have seen that the transform T has only one attractor, namely its fixed point $x=1$. This implies (Fatou 1919, 1920) that J is a Cantor set of the negative real axis. We shall present a picture of this set in § 3. Since J is real every point $\mathrm{i}\omega/\omega_0$ for $\omega\neq 0$ and ∞ is outside J, and therefore we get from (2.2):

$$\lim_{n\to\infty} Z_n(\omega)=(\mathrm{i}C_0\omega)^{-1} \qquad \text{for } \omega\neq 0 \text{ and } \infty \tag{2.6}$$

but this limit is far from being uniform in ω and $Z_n(\omega)$ exhibits interesting scaling

behaviours when $\omega \to 0$ or ∞ and $n \to \infty$ simultaneously. We shall return to this in §§ 2.1.2 and 2.1.3.

2.1.1. DC *response.* The DC response of our DFL is clearly given by equation (2.2) in the $\omega \to 0$ limit, where the transform T can be replaced by its linear approximation:

$$x \to \mu_0 x \qquad \text{with} \qquad \mu_0 = \frac{dT}{dx}(0) = \frac{f}{2f-1} \tag{2.7}$$

and hence:

$$Z_n = \mu_0^n R_0. \tag{2.8}$$

As expected we get a pure resistance at each generation. In order to give a physical meaning to the factor μ_0^n, let us introduce the total length L of the DFL between points A and B

$$L = 2^n. \tag{2.9}$$

Using this formula, we get an exact expression of the resistance $R = Z_n(\omega = 0)$ of the lattice as a function of its length only:

$$R = R_0 L^{t/\nu} \tag{2.10}$$

with

$$t/\nu = \ln \mu_0 / \ln 2. \tag{2.11}$$

We have identified the exponent in equation (2.10) with the ratio of the critical indices t and ν of percolation, by using the standard finite size scaling law, which is not problematic below dimension 6, and which has been extensively used in numerical determinations of the exponents s and t (Derrida *et al* 1983b, Herrmann *et al* 1984, etc...).

Equation (2.11) relates the exponent t/ν of the DFL to the parameter f, which did not receive any interpretation up to here. The original choice of Kirkpatrick was $f = \frac{3}{4}$, which leads to $t/\nu = 0.585$. One could use equation (2.11) and the known value: $t/\nu = s/\nu = 0.977$ (Zabolitzky 1984, Hong *et al* 1984, Herrmann *et al* 1984) to get:

$$f = 0.670. \tag{2.12}$$

This will indeed be our method of optimising f in the 3D case. However we have another criterion to determine the optimal value of f, namely to require that the lattice is *self-dual.* We know that the self-duality of a 2D square lattice has very interesting consequences in percolation, the most famous one being the equality $s = t$. Since the conductances of two dual bonds are reciprocals of each other, the DFL is self-dual if we have:

$$T[x]T[1/x] = 1 \qquad \text{for all } x. \tag{2.13}$$

It is straightforward to check that this holds for

$$f = \tfrac{2}{3}. \tag{2.14}$$

Let us mention that it was not obvious (at least to us) that the DFL was self-dual for a particular choice of its parameter f. We shall comment on the very tiny difference between the two values (2.12) and (2.14) in the next subsection. Throughout the following, most equations contain f as a free parameter, but we use the self-dual value (2.14) for figures, and for comparison with realistic situations.

2.1.2. Scaling behaviour at $\omega \to 0$. Consider the impedance $Z_n(\omega)$ given by equation (2.2) when $n \to \infty$ and $\omega \to 0$. This region has to exhibit a non-trivial crossover, since we know that $Z_n(\omega) \to (iC_0\omega)^{-1}$ (2.6) when $n \to \infty$ first; $Z_n(\omega) = \mu_0^n R_0$ (2.8) when $\omega \to 0$ first.

The DFL is simple enough to allow for a rigorous derivation of the scaling behaviour of $Z_n(\omega)$. For that purpose define the following *linearising variable*:

$$F_0(x) = \lim_{m\to\infty} T^m[x\mu_0^{-m}] \tag{2.15}$$

with μ_0 as in (2.7). It is easy to realise that F_0 satisfies the functional equation

$$F_0(\mu_0^n x) = T^n[F_0(x)] \tag{2.16}$$

for arbitrary integer n. We shall use the following properties of F_0: it is analytic around $x = 0$:

$$F_0(x) \underset{x\to 0}{=} x - f^{-1}x^2 + \dots \tag{2.17}$$

but singular around $x = \infty$:

$$F_0(x) \underset{\substack{x\to\infty \\ |\mathrm{Arg}\, x| < \pi}}{=} 1 + K_0 x^{-\Delta_0} + \dots . \tag{2.18}$$

The exponent Δ_0 is given by:

$$\Delta_0 = -\ln f / \ln \mu_0 \tag{2.19}$$

and K_0 is some f-dependent real number.

An easy way to derive (2.19) is for instance to insert (2.18) into (2.16) and use $dT(1)/dx = f$. Consider now a frequency such that $\omega \ll \omega_0$, and apply (2.16) to $x = i\omega/\omega_0$. We have asymptotically:

$$Z_n(\omega) = (iC_0\omega)^{-1} F_0(i\mu_0^n \omega/\omega_0). \tag{2.20}$$

By replacing n by its expression (2.9) in terms of L, one gets the following scaling behaviour for $\omega \ll \omega_0$ and $n \gg 1$:

$$Z_n(\omega) = R_0 L^{t/\nu} G_0[(\omega/\omega_0) L^{t/\nu}] \tag{2.21}$$

with $G_0(x) = (1/ix) F_0[ix]$.

Before giving the physical consequences of equation (2.21), let us mention that a very analogous scaling form for $Z_n(\omega)$ at $\omega \gg \omega_0$ and $n \gg 1$ can be derived through the same scheme. The result reads:

$$Z_n(\omega) = R_0 L^{-1} G_\infty[(\omega/\omega_0) L^{-1}] \tag{2.22}$$

where $G_\infty[x] = (1/ix) F_\infty[ix]$, and $F_\infty[x]$ is the linearising variable defined by:

$$F_\infty[x] = \lim_{m\to\infty} T^m[x\mu_\infty^{-m}] \tag{2.23}$$

($\mu_\infty = dT[\infty]/dx = \frac{1}{2}$ for all f). The function F_∞ is regular around $x = \infty$:

$$F_\infty[x] \underset{x\to\infty}{=} x + [2(1-f)]^{-1} + \dots \tag{2.24}$$

but singular around $x = 0$

$$F_\infty[x] \underset{\substack{x\to 0 \\ |\mathrm{Arg}\, x| < \pi}}{=} 1 + K_\infty x^{\Delta_\infty} \tag{2.25}$$

where K_∞ is some f-dependent real number, and where Δ_∞ is given by:

$$\Delta_\infty = -\ln f / \ln 2. \tag{2.26}$$

The exponent (-1) of the size L in equation (2.22) is to be interpreted as follows. Since $\omega \to \infty$ corresponds to a regime where capacitors are very good conductors, the resistance of the DFL at $\omega = \infty$ is expected to vanish as

$$Z_n[\infty] \sim L^{-s/\nu} \tag{2.27}$$

where s is the well known exponent of the supraconductivity problem, which also characterises the static dielectric constant. Since the function G_∞ goes to unity as $\omega \to \infty$, we deduce from (2.22) that:

$$s/\nu = 1 \qquad \text{for all } f. \tag{2.28}$$

The DFL has therefore the particularity that t/ν depends continuously upon f (see (2.11)) while s/ν is independent of f. The self-dual value $f = \frac{2}{3}$ naturally gives $t/\nu = s/\nu = 1$. Since the value of $t/\nu = s/\nu$ is very close to unity in real 2D systems (cf introduction), the value (2.12) of f happens to be very close to $f = \frac{2}{3}$.

The DFL has another striking feature: for percolation on regular lattices, the scaling laws of $Z(p, \omega)$ for $p \to p_c$ and $\omega \to 0$ and ∞ are expected to read respectively:

$$\begin{aligned} Z(p,\omega) &\underset{\substack{p\to p_c\\ \omega\to 0}}{=} (p-p_c)^t \rho_0[\mathrm{i}(\omega/\omega_0)(p-p_c)^{-s-t}] \\ Z(p,\omega) &\underset{\substack{p\to p_c\\ \omega\to \infty}}{=} (p-p_c)^{-s} \rho_\infty[\mathrm{i}(\omega/\omega_0)(p-p_c)^{+s+t}] \end{aligned} \tag{2.29}$$

while the exponents s and t never mix on the DFL: only t/ν appears as $\omega \to 0$ (2.21) and only s/ν as $\omega \to \infty$ (2.22).

Another way to put it is to compute the static dielectric constant:

$$\varepsilon = \lim_{\omega \to 0} \frac{1}{\omega} \operatorname{Im} \frac{1}{Z(\omega)}. \tag{2.30}$$

From equations (2.17) and (2.21), we deduce easily that this quantity is *finite* as $L \to \infty$ on the DFL:

$$\varepsilon = \frac{C_0}{f} \tag{2.31}$$

while it is expected to diverge as $p \to p_c$ in real systems as

$$\varepsilon \sim |p - p_c|^{-s} \tag{2.32}$$

This peculiarity of our model seems to be physically due to the fact that the DFL mimics rather a *bare* backbone than a full percolating lattice with its whole distribution of finite clusters. It is indeed clear that the DFL possesses no finite cluster of resistors and the critical enhancement (2.32) of the static dielectric constant, which occurs in both phases $p > p_c$ and $p < p_c$, is due to the divergent size of finite conducting clusters. In any case, the exact result (2.31) is a limitation of the validity of our model.

2.1.3. The loss angle. The loss angle $\delta(\omega)$ is defined by the following equation:

$$\tan \delta = -\mathrm{Re}[z]/\mathrm{Im}[z] \tag{2.33}$$

It has the advantages of being both a dimensionless quantity, and of being directly accessible in experimental situations (Laugier 1982).

From the results of § 2.12 (equations (2.15) to (2.26)) we conclude that this angle has *four* different regimes as ω ranges from 0 to ∞, namely:

$$\text{(a)}\ \ \omega \ll \omega_0 L^{-t/\nu} \qquad \tan\delta = f L^{-t/\nu}\omega_0/\omega \tag{2.34a}$$

$$\text{(b)}\ \ \omega_0 L^{-t/\nu} \ll \omega \ll \omega_0 \qquad \tan\delta = A_0(\omega_0/\omega)^{\Delta_0} \tag{2.34b}$$

$$\text{(c)}\ \ \omega_0 < \omega \ll \omega_0 L \qquad \tan\delta = A_\infty(\omega/\omega_0)^{\Delta_\infty} \tag{2.34c}$$

$$\text{(d)}\ \ \omega \gg \omega_0 L \qquad \tan\delta = 2(1-f)(\omega/\omega_0)L^{-1}. \tag{2.34d}$$

The numbers A_0, A_∞ are given by:

$$\begin{aligned} A_0 &= -K_0 \sin(\tfrac{1}{2}\pi\Delta_0) L^{-\Delta_0 t/\nu} \\ A_\infty &= K_\infty \sin(\tfrac{1}{2}\pi\Delta_\infty) L^{-\Delta_\infty}. \end{aligned} \tag{2.35}$$

In order to see how far these asymptotic behaviours are reached for a finite generation n, we present in figure 3 a log-log plot of $\tan\delta$ against ω/ω_0 for $n = 1$-26. Since we have chosen the self-dual value $f = \frac{2}{3}$, the graph is symmetric with respect to the y axis. In particular the slopes Δ_0 and Δ_∞ are equal

$$\Delta_0 = \Delta_\infty = \ln\tfrac{3}{2}/\ln 2 = 0.585 \qquad \text{for } f = \tfrac{2}{3}. \tag{2.36}$$

The four expected slopes are clearly visible.

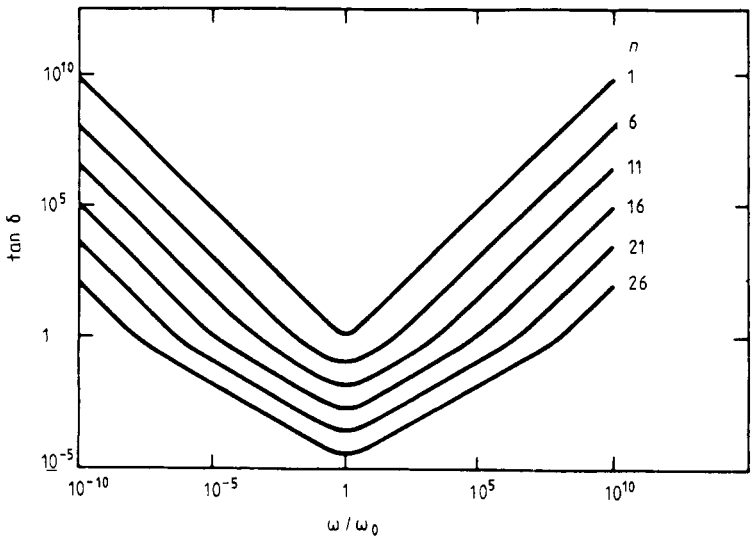

Figure 3. A log-log plot of $\tan\delta$ against ω/ω_0 for the self-dual DFL at generation $n = 1$ to 26.

2.2. Three-dimensional case

The iterative construction we have described in the introduction can be easily generalised to build a DFL in arbitrary dimension $D > 2$. To do so, one considers cells containing $2D$ bonds, since $2D$ is the scaling factor of a volume when the linear scale is doubled. Since we are mostly interested in 3D situations, we shall describe our

construction scheme in that case. Figure 4 shows the generations $n=0$, 1 and 2 of the 3D DFL in the case $f=\frac{5}{8}$ (just in order to have integer numbers of resistors and capacitors). As in the 2D case, we allow for a continuously varying conducting fraction f in the following way: the upper half of each cell contains four bonds, among which $8(1-f)$ are capacitors, and hence $8f-4$ are resistors; the lower half is still purely resistive. We shall restrict ourselves to values of f lying in the interval: $\frac{1}{2}<f<1$

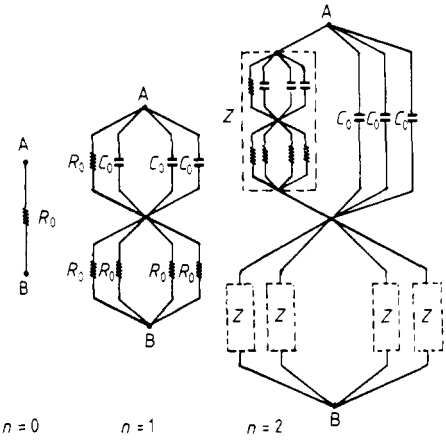

Figure 4. The circuit representation of the 3D DFL at generation $n=0$, 1, 2, for $f=\frac{5}{8}$.

In complete analogy with the 2D case, and with the same notation, the impedance $Z_n(\omega)$ of the 3D DFL satisfies the following recursion relation:

$$Z_n(\omega)=\tfrac{1}{4}Z_{n-1}(\omega)+\left(\frac{8(1-f)}{\zeta(\omega)}+\frac{8f-4}{Z_{n-1}(\omega)}\right)^{-1} \tag{2.37}$$

where $\zeta(\omega)=(\mathrm{i}C_0\omega)^{-1}$ still denotes the impedance of one capacitor.

In the limiting case $f=1$ of a *pure* resistive medium, the resistance R_n of the whole DFL reads therefore: $R_n=2^{-n}R_0$. The factor 2^{-n} is due to the fact that for $D=2$ we must distinguish between resistance and resistivity. In order to take this trivial geometrical factor into account, let us define the frequency-dependent resistivity $z_n(\omega)$ through

$$Z_n(\omega)=2^{-n}z_n(\omega). \tag{2.38}$$

It is now very easy to iterate equation (2.37) down to $n=0$ and to get:

$$z_n(\omega)=(\mathrm{i}C_0\omega)^{-1}T^n(\mathrm{i}\omega/\omega_0). \tag{2.39}$$

The expression of $z_n(\omega)$ in the 3D DFL is *identical* to that of Z_n in the 2D case. The very same transformation T holds for all dimensionalities. The only parameter which varies with dimension is of course f: we shall find the optimal f in the 3D case in a while.

The properties of the mapping T we have used in the 2D case are naturally still useful. Therefore, in the rest of this section we shall only mention the numerical values of those quantities which are different in dimensions 2 and 3.

2.2.1. DC response. In analogy with the 2D case, we obtain the following expression for the resistivity $\rho=z_n(0)$ of the DFL as a function of its length:

$$\rho=R_0L^{t/\nu} \tag{2.40}$$

where t/ν is still related to f through equations (2.7)-(2.11). The known value of this exponent ratio for percolation on a regular 3D lattice ($t/\nu = 2.20 \pm 0.10$: Derrida *et al* 1983b) determines the optimal value of our parameter f:

$$f = 0.561. \tag{2.41}$$

2.2.2. The loss angle. The four regimes in the frequency dependence of the loss angle δ, described in equation (2.34), still hold in the 3D case. The numerical values of the exponents Δ_0, Δ_∞ read (for $f = 0.561$):

$$\Delta_0 = 0.379 \qquad \Delta_\infty = 0.834. \tag{2.42}$$

Since these exponents obey the relation:

$$\Delta_0/\Delta_\infty = s/t \tag{2.43}$$

for all f, which is a consequence of their definition, it is not surprising that they are different from each other. Just as in the 2D case, figure 5 shows a log-log plot of $\tan\delta$ against (ω/ω_0) for $n = 1$ to 21. The four asymptotic slopes are again clearly visible.

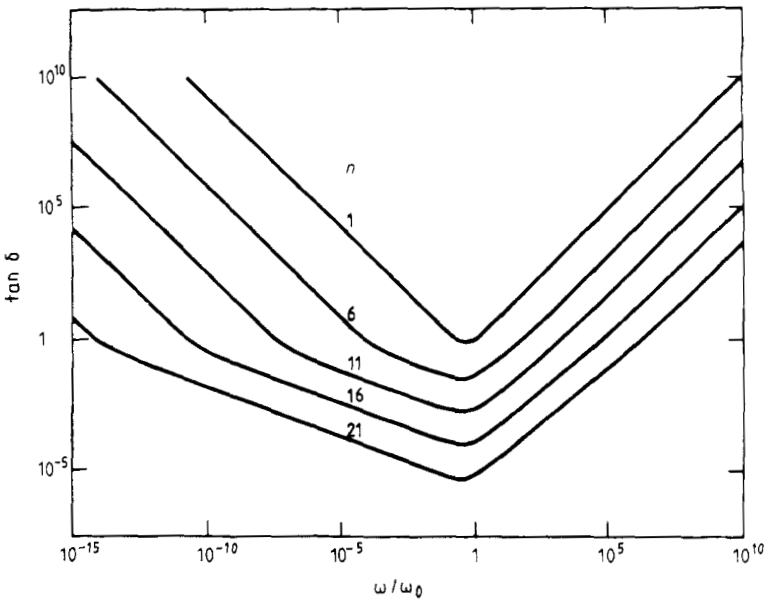

Figure 5. A log-log plot of $\tan\delta$ against ω/ω_0 for the 3D DFL ($f = 0.561$) at generation $n = 1$-21.

3. Response to an arbitrary signal

In this section, we shall study the electrical response of the DFL to an arbitrary potential difference $V(t)$ between its end-points A and B. This response may be characterised by several different quantities: intensity in a given branch of the network, total dissipated power, etc.... We have chosen for simplicity the voltage $F_n(t)$ across one of the capacitors which appears at generation $n = 1$. Figure 6 shows the circuit corresponding to the $(n+1)$th generation of the whole 2D DFL, for $f = \frac{3}{4}$.

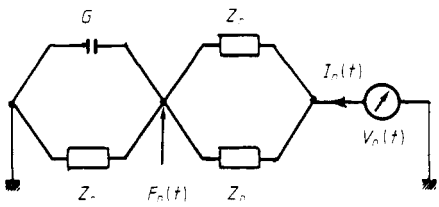

Figure 6. Definition of the response voltage $Fn(t)$ of the DFL to an arbitrary input signal t.

The computation of $F_n(t)$ we present here is valid for all f and arbitrary dimension. We shall do it in detail in the 2D case, and let the reader convince himself that our result (3.2) is also valid in the 3D case.

Let $\tilde{V}$, $\tilde{I}_n(\omega)$ and $\tilde{F}_n(\omega)$ denote the Fourier transforms of the input signal $V(t)$, the global intensity across the DFL, and our response signal respectively. They are related through:

$$\tilde{I}_n(\omega)=\frac{\tilde{V}(\omega)}{Z_{n+1}(\omega)}=\tilde{F}_n(\omega)\left(\frac{4(1-f)}{\zeta(\omega)}+\frac{4f-2}{Z_n(\omega)}\right). \tag{3.1}$$

Using the expression (2.2) of the impedance $Z_n(\omega)$, we obtain the following equation:

$$\tilde{F}_n(\omega)=\tilde{V}(\omega)\tfrac{1}{2}[(1-f)T^n(\mathrm{i}\omega/\omega_0)+f]^{-1} \tag{3.2}$$

which solves our problem: the response $\tilde{F}_n(\omega)$ is expressed as a function of the input $\tilde{V}(\omega)$. In order to illustrate the general features of this response, which are contained in the right-hand side of equation (3.2), let us take the example of a step-function input

$$\begin{aligned} V(t)&=V_0\theta(t)\\ \tilde{V}(\omega)&=V_0\mathrm{i}(\omega-\mathrm{i}0). \end{aligned} \tag{3.3}$$

The signal $F_n(t)$ is then given by the following integral:

$$F_n(t)=\int\frac{\mathrm{d}\omega}{2\pi\mathrm{i}}\,\frac{\mathrm{e}^{\mathrm{i}\omega t}}{\omega-\mathrm{i}0}\,\frac{V_0}{2[(1-f)T^n(\mathrm{i}\omega/\omega_0)+f]}. \tag{3.4}$$

For $n=0$, the integral is easily evaluated by closing the contour in the lower half plane for $t<0$:

$$F_0(t)=0 \tag{3.5a}$$

and in the upper half plane for $t>0$:

$$F_0(t)=(V_0/2f)[1-\exp(-f\omega_0 t/1-f)]. \tag{3.5b}$$

This result could of course be obtained by elementary circuit equations. The basic feature of this expression is the occurrence of one relaxation time τ given by:

$$\omega_0\tau=\frac{1-f}{f}. \tag{3.6}$$

For arbitrary n, the same way of closing integration contours and summing residues leads to the following expressions of $F_n(t)$ for $t<0$:

$$F_n(t)=0 \tag{3.7a}$$

and for $t>0$:

$$\frac{F_n(t)}{V_0}=\frac{1}{2f}+\frac{1}{2(1-f)}\sum_{1\leqslant a\leqslant 2^n}\frac{\exp(x_a\omega_0 t)}{x_a(\mathrm{d}T^n[x_a]/\mathrm{d}x)} \tag{3.7b}$$

where the integer a labels the pre-images x_a of the point $f/(f-1)$ by the 2^n branches of T^{-n}, and where $\mathrm{d}T^n[x_a]/\mathrm{d}x$ denotes the derivative of the direct mapping T^n at those points. Since the point $f/(f-1)$ satisfies:

$$T\left[\frac{f}{f-1}\right]=0 \tag{3.8}$$

and since the origin belongs to the Julia set J (see § 2.1), we deduce that $f/(f-1)$ and all the x_a also belong to the Julia set of T. In particular, the x_a are real negative numbers. In other words, the right-hand side of equation (3.7*b*) is a sum of 2^n purely exponentially decreasing functions.

The DFL at generation n possesses 2^n intrinsic relaxation times simply related to the x_a:

$$\tau_a^{-1}=-x_a\omega_0. \tag{3.9}$$

For instance, for $f=\frac{2}{3}$ in the 2D case, the x_a read:

$$\begin{aligned}
&n=0 \qquad -x_1=2\\
&n=1 \qquad -x_1=0.354\,249\\
&\qquad\quad -x_2=5.645\,751\\
&n=2 \qquad -x_1=0.137\,803\\
&\qquad\quad -x_2=0.439\,282\\
&\qquad\quad -x_3=2.570\,695\\
&\qquad\quad -x_4=12.852\,220
\end{aligned} \tag{3.10}$$

etc.

When the size of the DFL becomes large, we know that the 2^n points x_a converge towards the whole Julia set J of the mapping T, and that their density converges towards the unique balanced invariant measure on this set denoted $\mathrm{d}\mu$ (Brolin 1965, Barnsley *et al* 1982). This invariant measure plays a crucial role in the theory of rational transformations and Julia sets. We shall not need many of its properties in the following, except the fact that the 2^n relaxation times given by (3.9) converge towards the Julia set J, independently of the input signal $V(t)$, and their density on that set is also given by the remarkable mathematical objects $\mathrm{d}\mu$, independently of $V(t)$. In particular, since J extends from 0 to ∞, the infinite DFL exhibits arbitrarily small and large time scales. For a large but finite generation n, it is easy to realise that the smallest and largest relaxation times behave like:

$$(\omega_0\tau_s)^{-1}\simeq C_s L \tag{3.11a}$$

$$(\omega_0\tau_l)^{-1}\simeq C_l L^{-t/\nu} \tag{3.11b}$$

where C_s and C_l are f-dependent numbers, which happen to be related to the linearising variables F_0 and F_∞ of § 2.1.2. More precisely, $-C_l$ is the location of the singularity of F_0 having the smallest modulus, $-C_s$ is the location of the singularity of F_∞ having the largest modulus.

In percolation on regular lattices, the largest time scale is expected to diverge when $p \to p_c$ as

$$\tau_1 \sim |p - p_c|^{-(s+t)}. \tag{3.12}$$

The fact that t appears in equation (3.11b) instead of $(s+t)$ has already been mentioned in § 2.1.2. The existence of relaxation times much smaller than $\omega_0^{-1} = R_0 C_0$ may appear more astonishing, since $R_0 C_0$ sets the microscopic time scale of the DFL. However it is easy to realise that the very particular geometry of the DFL is responsible for these very quick transport phenomena. For instance, the capacitors we are looking at receive or loose charges through 2^n resistances R_0 in parallel, giving rise to time scales as small as $\tau_s \sim 2^{-n}$.

The co-existence of small and large relaxation times is illustrated in figure 7, which shows a plot of $F_n(t)$ for $n = 0$-3, and $f = \frac{2}{3}$ corresponding to an input $V(t) = \theta(t)$.

It is clear that, as n increases, the beginning of the response signal gets steeper and steeper while its long time tail stretches farther and farther.

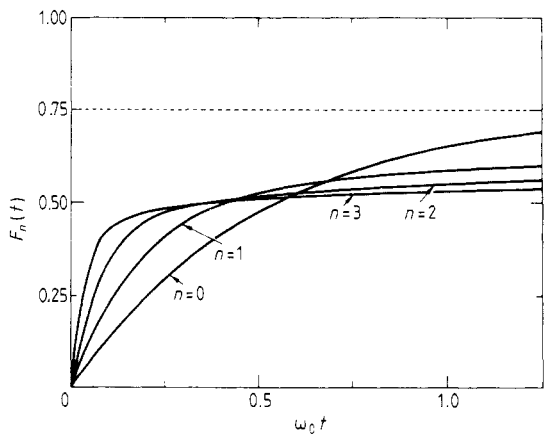

Figure 7. The response signal $F_n(t)$ as a function of time, for $f = \frac{2}{3}$ and $n = 0$ to 3. The input is a unit step function ($V_0 = 1$).

Figure 8 shows a part of the Julia set J for $f = \frac{2}{3}$. The integrated density $H(x)$ of the invariant measure $d\mu$:

$$H(x) = \mu(]-\infty; x[) \tag{3.13}$$

is plotted against x, for $-10 < x < 0$.

In other words, the continuous function $H(x)$ represents the fraction of relaxation times which are less than x for a very large DFL. $H(x)$ is non-zero for arbitrary large negative values of x, since we have seen that the (infinite) DFL possesses arbitrarily small relaxation times. $H(x)$ also exhibits interesting scaling behaviour as $x \to 0$ or $x \to -\infty$, that we shall need not hereafter, and therefore do not, discuss for sake of brevity. Each interval where H is a constant is a hole of J. Between any two points x_1 and x_2 with $H(x_1) \neq H(x_2)$ there exists one point of J, and therefore an infinity of them. This plot gives a feeling of the complexity of the relaxation times of the (infinite) DFL.

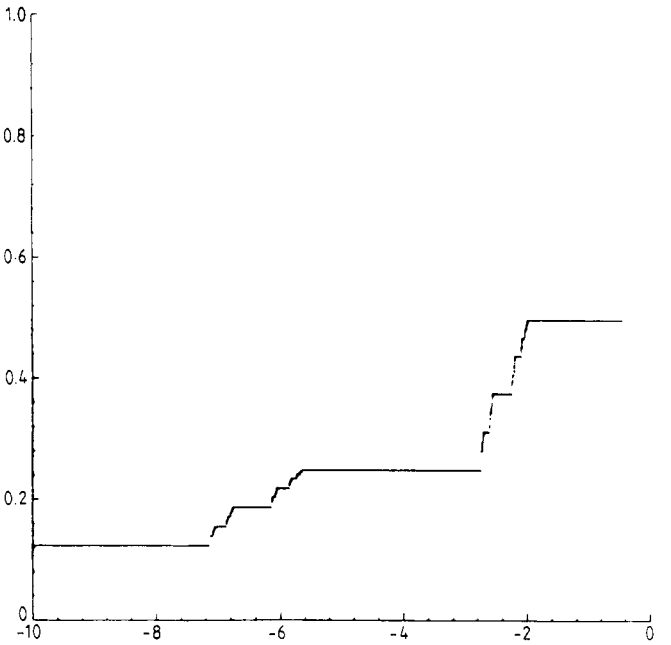

Figure 8. An illustration of the Julia set J associated to the mapping T for $f=\frac{2}{3}$, showing the integrated density $H(x)$ of the invariant measure $d\mu$ for $-10<x<0$.

4. The problem of noise

Another question of interest can be exactly solved on the DFL: what is the observable noise spectrum of the whole lattice if each resistor has a given noise? Let us assume that the resistance of each conducting bond has a small time-dependent dimensionless random component $\Delta_0(t)$:

$$R = R_0|1+\Delta_0(t)|. \tag{4.1}$$

These fluctuations are assumed to be identical, stationary independent of each other, and characterised by their common spectral density:

$$S_0(\omega) = \int \mathrm{d}t\, \mathrm{e}^{\mathrm{i}\omega t}\langle\Delta_0(t)\Delta_0(0)\rangle. \tag{4.2}$$

This models the so-called flicker noise, which happens to be in $1/f$ (i.e. $S_0(\omega)\sim 1/\omega$) in most cases.

Let us first consider the 2D lattice. In that case, the noise spectrum of the whole DFL at generation $n=1$ is obtained as follows: starting from equation (4.1) for each of the $4f$ resistors of the cell, one looks for the renormalised noise $\Delta_1(t)$ such that the impedance $Z_R(\omega)$ of the whole lattice between A and B reads:

$$Z_R(\omega) = Z_1(\omega)[1+\tilde{\Delta}_1(\omega)] \tag{4.3}$$

where we have used the Fourier transform in order not to write time integrals and derivatives. The resulting spectral density $S_1(\omega)$ is then obtained through its definition, in analogy with (4.2):

$$S_1(\omega) = |\tilde{v}_1(\omega)|^2. \tag{4.4}$$

The result is:

$$S_1(\omega) = S_0(\omega) g(i\omega/\omega_0) \tag{4.5}$$

where the gain (or amplification) g is the following f-dependent function:

$$g(x) = \frac{2f-1+|2(1-f)x+2f-1|^4}{8|(1-f)x+f|^2|2(1-f)x^2+2f-1|^2}. \tag{4.6}$$

This computation can be easily pursued up to an arbitrary generation n, where the noise spectrum of the whole DFL reads:

$$S_n(\omega) = S_0(\omega) g(i\omega/\omega_0) g[T(i\omega/\omega_0)] \ldots g[T^{n-1}(i\omega/\omega_0)]. \tag{4.7}$$

Since we are interested in the frequency dependence of this noise spectrum, let us define the *relative* amplification $\Gamma_n(\omega/\omega_0)$ by dividing each g function in (4.7) by the constant factor $g(1) = f/4$:

$$\Gamma_n\left(\frac{\omega}{\omega_0}\right) = \left(\frac{4}{f}\right)^n \frac{S_n(\omega)}{S_0(\omega)} = \prod_{0 \le k \le n-1} \frac{4}{f} g[T^k(i\omega/\omega_0)]. \tag{4.8}$$

This definition ensures that Γ_n has a smooth limit $\Gamma_\infty(\omega/\omega_0)$ when $n \to \infty$, for $\omega \neq 0$ and ∞. This limit, which describes the frequency dependence of the noise amplification of the infinite DFL, obeys the following functional equation:

$$\Gamma_\infty(\omega/\omega_0) = f^{-1} g(i\omega/\omega_0) \Gamma_\infty[-iT(i\omega/\omega_0)]. \tag{4.9}$$

From this exact relation, we deduce in particular the behaviour of the noise amplification at low frequency:

$$\Gamma_\infty(\omega/\omega_0) \underset{\omega \to 0}{\sim} (\omega/\omega_0)^{-Y_0} \tag{4.10a}$$

with

$$Y_0 = \frac{\ln 4g(0)/f}{\ln \mu_0} \tag{4.10b}$$

and at high frequency:

$$\Gamma_\infty(\omega/\omega_0) \underset{\omega \to \infty}{\sim} (\omega/\omega_0)^{-Y_\infty} \tag{4.11a}$$

with

$$Y_\infty = \frac{\ln 2/f}{\ln 2}. \tag{4.11b}$$

The noise amplification exhibits therefore a power-law behaviour for $\omega \ll \omega_0$ and $\omega \gg \omega_0$. At $\omega = 0$, $\Gamma_n(\omega/\omega_0)$ diverges with the size of the DFL as:

$$\Gamma_n[0] = [4f^{-1} g(0)]^n = L^{Y_0 t/\nu}. \tag{4.12}$$

The problem of noise on the 3D DFL is soluble by the very same method. The only difference is that the function g defined in equation (4.6) contains an overall factor $\frac{1}{2}$:

$$g_{3D}[x] = \tfrac{1}{2} g_{2D}[x]. \tag{4.13}$$

This factor is cancelled out in the definition of the relative amplification $\Gamma_n(\omega)$, which has therefore the same properties in dimensions 2 and 3. In particular, the power laws (4.10)-(4.11) hold in arbitrary dimension.

If we take for f their optimal values in the 2D and 3D models, the noise exponents read:

$$\begin{array}{lllll} \text{2D} & [f=\frac{2}{3}] & Y_0=2.392 & Y_\infty=1.585 \\ \text{3D} & [f=0.561] & Y_0=2.062 & Y_\infty=1.834. \end{array} \tag{4.14}$$

The fact that noise amplification exhibits scaling behaviours with its own critical exponents (Y_0, Y are not (simply) related to s and t) has also been recently pointed out by Rammal (1984), Luck (1984) and Rammal *et al* (1985). The fact that Y is related to the fractal dimension d_f of our DFL (see equation (5.3) in next section) through $Y = Y_\infty = 1 - D + d_f$, is merely a coincidence due to the simplicity of our model, just as the result $s = \nu$ (see equation (2.28)), and by no means a genuine equality between critical exponents.

The fact that Γ_∞ diverges at $\omega \to \infty$ with the positive exponent Y_∞ is not surprising if we remember that we deal with the amplification of the *dimensionless* quantity $\Delta(t)$ normalised with respect to the *total impedance* of the DFL which falls off as $1/\omega$.

5. Remarks and conclusion

We have shown that the original Kirkpatrick deterministic model of a 2D percolation backbone is easily generalisable to time-dependent electrical properties, and to dimensionalities $D > 2$. The presence of the free parameter f in the model is crucial: otherwise all properties would be independent of dimension. In the 2D case, our DFL is self-dual for the particular value $f = \frac{2}{3}$, where we have $s/\nu = t/\nu = 1$, while the value 0.977 is expected on real systems. In the 3D case, where we have no simple geometrical criterion to choose an optimal value of f, the fit of t/ν with its (numerically) known value seems reasonable.

A considerable advantage of the DFL is that a complete analytical treatment of a large number of properties is available. The basic difference between our model and percolation clusters has been pointed out in § 2.1.2: its static dielectric constant does not diverge with the size of the DFL. This lack of a singularity has several implications: the length-frequency crossover exponent is t/ν instead of $(s+t)/\nu$; the loss angle δ has a minimum about $\omega = \omega_0$ which goes to zero as f^n when $n \to \infty$, while this minimum is expected to reach the following universal value in realistic systems:

$$\delta_c = \frac{\pi}{2}\frac{s}{s+t}. \tag{5.1}$$

This relation is a consequence of the scaling laws (2.29), where ρ_0 and ρ_∞ are real analytic functions. The physical origin of this difference is probably the absence of finite clusters around the infinite one: in a loose sense the DFL is a bare backbone.

Our model can be generalised to more complicated bonds than pure resistors and capacitors. Experimentally interesting situations correspond for instance to a frequency-dependent resistance of the conducting bonds, taking into account the skin conductance at high frequency, or the detailed texture of the microbeads in experiments on powders (Laugier 1982). Let us describe in more detail a special choice of bond impedances which gives rise to a *chaotic behaviour*. Assume that the resistors are replaced by pure inductances L_0 (impedance $iL_0\omega$) while the capacitors remain perfect (impedance $(iC_0\omega)^{-1}$). A simple modification of equation (2.2) gives the following

expression for the impedance of the 2D DFL:

$$Z_n(\omega) = (iC_0\omega)^{-1} T^n(-\omega^2/\omega_0^2) \tag{5.2}$$

where $\omega_0^2 = (L_0 C_0)^{-1}$. Since there are no losses in the system, Z_n is purely imaginary. Its ω dependence can be said to be chaotic in the following sense. There exist 2^n (real positive) values of ω^2 where $Z_n(\omega)$ vanishes (so that $(-\omega^2/\omega_0^2)$ is a pre-image of 0 by T^{-n}) and 2^n other values of ω^2 where $Z_n(\omega)$ is infinite (like $(-\omega^2/\omega_0^2)$ is a pre-image of ∞ by T^{-n}). These two series of points are contained in the Julia set of transformation T. The impedance $Z_n(\omega)$ has therefore a smooth behaviour when $(-\omega^2/\omega_0^2)$ describes the holes of J, but undergoes wild variations (for large n) when $(-\omega^2/\omega_0^2)$ crosses J.

Let us finally emphasise that the DFL certainly does not reproduce correctly all properties of percolation clusters which are related to the structure of the backbone, since the exponents s and t are far from being sufficient to characterise a fractal set. More subtle problems, like elasticity or viscosity, certainly require a more delicate treatment. We just mention a simple quantity, namely the Hausdorff (or fractal) dimension, with which the values on the DFL and on a percolating backbone are not in a good agreement. Since the conducting part of the DFL is made of $4f$ (respectively $8f$) parts which are similar to it in the 2D (respectively 3D) model, with a similarity ratio $\frac{1}{2}$, the fractal dimension of the DFL reads:

$$\begin{aligned} &\text{2D} \qquad d_f = (\ln 4f)/(\ln 2) = 1.415 \\ &\text{3D} \qquad d_f = (\ln 8f)/(\ln 2) = 2.166. \end{aligned} \tag{5.3}$$

These numbers are to be compared with the recent accurate numerical work of Puech and Rammal (1983) which predicts:

$$\text{2D} \qquad d_f = 1.68 \pm 0.02 \tag{5.4a}$$

and that of Herrmann and Stanley (1984) which predicts:

$$\begin{aligned} &\text{2D} \qquad d_f = 1.62 \pm 0.02 \\ &\text{3D} \qquad d_f = 1.74 \pm 0.04. \end{aligned} \tag{5.4b}$$

This illustrates once more that percolating clusters cannot be reduced to a small collection of exponents.

It would be very interesting to compare the predictions of the present study of the DFL with experimental data and theoretical work on more realistic systems. Let us mention that one of us (Luck 1985) has used the Migdal-Kadanoff approximation (or equivalently hierarchical lattices) to examine the same kind of problems in 2D and 3D percolation clusters, in particular the loss angle, and the low-frequency noise amplification.

Acknowledgments

It is a pleasure to thank B Derrida, H J Herrmann and R Rammal for fruitful discussions.

References

Alexander S and Orbach R 1982 *J. Physique Lett.* **43** L625
Barnsley M F, Geronimo J S and Harrington A N 1982 *Bull. Am. Math. Soc.* 7 381

Brolin H 1965 *Ark. Math.* **6** 103
Clerc J P, Tremblay A M S, Albinet G and Mitescu C D 1984 *J. Physique Lett.* **45** L913
Derrida B, Itzykson C and Luck J M 1984 *Commun. Math. Phys.* **94** 115
Derrida B, de Seze L and Itzykson C 1983a *J. Stat. Phys.* **33** 559
Derrida B, Stauffer D, Herrmann H J and Vannimenus J 1983b *J. Physique Lett.* **44** L701
Essam.J W 1980 *Rep. Prog. Phys.* **43** 833
Fatou P 1919 *Bull. Soc. Math. France* **47** 161
—— 1920 *Bull. Soc. Math. France* **48** 33, 208
Gefen Y, Aharony A and Mandelbrot B B 1981 *Phys. Rev. Lett.* **47** 1771
Herrmann H J, Derrida B and Vannimenus J 1984 *Phys. Rev.* B **30** 4080
Herrmann H J and Stanley H E 1984 *Phys. Rev.* **53** 1121
Hong D C, Havlin S, Herrmann H J and Stanley H E 1984 *Phys. Rev.* B **30** 4083
Itzykson C and Luck J M 1983 *Proc. Brasov Int. School on Critical Phenomena: Theoretical Aspects* in press
Julia G 1918 *J. Math., Paris* sér. 7 **4** 47
Kirkpatrick S 1978 *Electrical Transport and Optical Properties of Inhomogeneous Media AIP Conf. Proc.* Vol 40 (New York: AIP) p 99
—— 1979 *Ill-condensed matter, Proc. Les Houches Summer school* ed R Balian, R Maynard and G Toulouse (Amsterdam: North-Holland)
Laugier J M 1982 *Thèse de 3ème cycle* Université de Provence, Marseille
Lobb C J and Franck D J 1984 *Phys. Rev.* B **30** 4090
Luck J M 1985 *J. Phys. A: Math. Gen.* **18** 2061
Mandelbrot B B 1982 *Fractal Geometry of Nature* (San Francisco: Freeman)
Puech L and Rammal R 1983 *J. Phys. C: Solid State Phys.* **16** L1197
Rammal R 1984 *J. Physique Lett.* **45** L1007
Rammal R, Tannous C, Breton P and Tremblay A M S 1985 to be published
Rammal R, Tannous C and Tremblay A M S 1984 *Phys. Rev.* A in press
Rammal R and Toulouse G 1983 *J. Physique Lett.* **44** L13
Stanley H E and Coniglio A 1984 *Phys. Rev.* B **29** 522
Stauffer D 1979 *Phys. Rep.* **54** 3
Zabolitzky J G 1984 *Phys. Rev.* B **30** 4077